A Novel Complex-Modulation Based Space-Time Spreading Scheme with More Than Two Transmit Antennas for MC-DS-CDMA Systems

Jia Tang and Xi Zhang
Networking and Information Systems Laboratory
Department of Electrical Engineering
Texas A&M University, College Station, TX 77843, USA
Email: {jtang, xizhang}@ee.tamu.edu

***Abstract*—Space-time spreading (STS) is a promising scheme combining the ubiquitously employed code division multiple access (CDMA) with the emerging space-time block coding (STBC) technique. Almost all research results reported so far mainly focus on the STS schemes based on the *full-rate* STBC, which use either only *two* transmit antennas or *real*-modulations. However, the *complex*-modulation based STS systems with more than two transmit antennas, despite their much better spectrum efficiency and error performance, hardly receive any attention. To remedy this deficiency, in this paper we propose a complex-modulation based STS scheme with more than two transmit antennas for MC-DS-CDMA systems. We also develop the performance analysis frameworks to evaluate the bit-error-rate (BER) and throughput of the proposed scheme and other representative schemes. The simulation results obtained verify the analytical findings. Both analytical and simulation results show that our proposed scheme can achieve much lower BER and much higher throughput as compared to their counterparts using real-modulation based STS systems.**

Keyword*—Space-Time Spreading (STS), Multicarrier-Direct-Sequence-CDMA (MC-DS-CDMA), Bit-error-rate (BER), Throughput analysis, Rayleigh fading channel.

I. INTRODUCTION

Multicarrier code division multiple access (MC-CDMA) integrating orthogonal frequency division multiplexing (OFDM) with spreading spectrum transmission emerges as a promising technique for the next-generation wireless communication systems [4][10]. A number of MC-CDMA schemes have been proposed including multi-tone (MT) DS-CDMA, MC-DS-CDMA, and MC-CDMA using the frequency domain spreading. Among them, MC-DS-CDMA, employing direct-sequence (DS) spreading in time domain for each subcarrier signal, is capable of circumventing many problems encountered by other CDMA schemes [9] and therefore receives much research attention.

On the other hand, a novel technique called space-time spreading (STS), which combines the widely adopted CDMA with space-time block coding (STBC), has recently received a great deal of research efforts [1][2][3][8][9]. STS was first proposed in [3] and thoroughly studied in [1] in the DS-CDMA context. In [9], STS is introduced to MC-DS-CDMA based systems. All the aforementioned works mainly focus on STS schemes based on the *full-rate* STBC, which employ either only *two* transmit antennas with both real- and complex-modulations [2][8] or *real*-modulations using an arbitrary number of transmit antennas [9]. We call this type of schemes the *full-rate STS*. However, there has been hardly any research reported on STS schemes based on the *non-full-rate* STBC, which use *complex*-modulation with more than two transmit antennas. We call this type of schemes the *non-full-rate STS*. The investigation on non-full-rate STS is of significant importance because the complex-modulations and increased space diversity due to more transmit antennas used can greatly improve the spectrum efficiency and error performance.

To remedy this deficiency, in this paper by using the half-rate STBC we propose an efficient complex-modulation based STS scheme with more than two transmit antennas for MC-DS-CDMA systems, which can achieve the same transmission rate without demanding extra bandwidth as compared to the full-rate STS schemes. We implement this scheme by just using one more spreading code, where each user is assigned two spreading codes. In addition, we develop the performance analysis frameworks to compare the bit-error-rate (BER) and throughput of the proposed scheme with those of the other existing schemes. The analytical results are verified by the extensive simulations. Both numerical and simulation results show that our proposed scheme can achieve much lower BER and much higher throughput as compared to its counterparts using the real-modulation based STS systems.

The paper is organized as follows. Section II describes the MC-DS-CDMA system model as well as the proposed complex-modulation based STS scheme. Section III derives the analytical performance frameworks to evaluate the BER and throughput of the proposed scheme and the other representative complex- and real-modulation based STS schemes. Section IV describes the analytical performance comparison and simulation results which confirm the analytical findings. The paper concludes with section V.

II. SYSTEM MODEL

In this paper, we consider the STS orthogonal MC-DS-CDMA system with N_T $(N_T > 2)$ antennas at the transmitter and N_R antennas at the receiver. The total number of orthogonal subcarriers is $V = U \cdot P$, which will be defined and described in the following section with more details. To simplify the presentation, we only investigate the scheme of single user transmission. However, the results derived from the single user case can be readily extended to the cases of multi-user synchronous transmissions.

A. Transmitter Model and Space-time Spreading Scheme

The structure of our proposed transmitter is shown in Fig. 1. A block of $P \cdot K$ complex-modulated symbols each with symbol duration of T_S is converted to P parallel sub-streams

This work reported in this paper was supported by the National Science Foundation CAREER Award under Grant ECS-0348694.

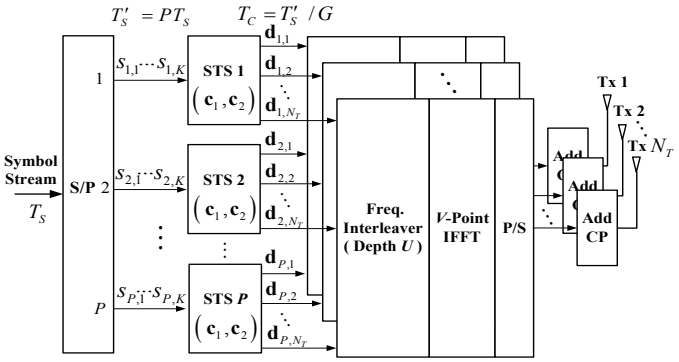

Fig. 1. Block diagram of the space-time spreading transmitter $(N_T > 2)$.

using Serial-to-Parallel (S/P) converter, where each sub-stream consists of K symbols. Thus, the symbol duration T_S' after S/P conversion becomes $T_S' = PT_S$. The pth sub-stream vector $\mathbf{s}_p$ consisting of K symbols can be expressed as $\mathbf{s}_p = \left(s_{p,1} \;\; s_{p,2} \;\; \ldots \;\; s_{p,K} \right)^T$, $p = 1,2,...P$, where $(\bullet)^T$ represents the transpose of $(\bullet)$. After S/P, each parallel sub-stream is space-time spreaded (STS) by 2 normalized orthogonal spreading codes $\mathbf{c}_1$ and $\mathbf{c}_2$, which are given by $\mathbf{c}_i = \left(c_{i,1} \;\; c_{i,2} \;\; \ldots \;\; c_{i,G} \right)^T$, $i = 1,2$, where G denotes the spreading gain of the codes. The codes satisfy $\mathbf{c}_k^H \mathbf{c}_l = \delta_{kl} \;\; \forall k,l = 1,2$, where $(\bullet)^H$ represents the conjugate-transpose of $(\bullet)$ and δ_{kl} is Kronecker Delta function. The chip duration T_C of the spreading codes satisfies $T_C = T_S'/G = PT_S/G$.

Without loss of generality, we choose $K = N_T = 4$ to present our proposed STS scheme. The proposed scheme and structure can be applied to other systems satisfying $K \geq N_T > 2$. For complex-modulated symbols belonging to the pth sub-stream, the half-rate STBC [6] is given by:

$$\tilde{\mathbf{S}}_p = \begin{pmatrix} \mathbf{S}_p \\ \mathbf{S}_p^* \end{pmatrix} \tag{1}$$

$$\text{where} \quad \mathbf{S}_p = \begin{pmatrix} s_{p,1} & s_{p,2} & s_{p,3} & s_{p,4} \\ -s_{p,2} & s_{p,1} & -s_{p,4} & s_{p,3} \\ -s_{p,3} & s_{p,4} & s_{p,1} & -s_{p,2} \\ -s_{p,4} & -s_{p,3} & s_{p,2} & s_{p,1} \end{pmatrix} \begin{matrix} \rightarrow \text{space}\,(N_T = 4) \\ \\ \\ \downarrow \;\; \text{time}\;\; (K = 4) \end{matrix} .$$

Theoretically [1], we need 8 different orthogonal codes each having a period of $4T_S'$ to realize STS, which implies that the scheme of one spreading code per user cannot satisfy the orthogonal requirement. Thus, we implement the STS scheme by using one extra spreading code. The 8-column spreading codes are arranged as follows:

$$\mathbf{C} = \left(\tilde{\mathbf{c}}_1 \;\; \tilde{\mathbf{c}}_2 \;\; \ldots \;\; \tilde{\mathbf{c}}_8 \right) = \begin{pmatrix} \mathbf{c}_1 & \mathbf{c}_2 & & & & & & \\ & & \mathbf{c}_1 & \mathbf{c}_2 & & & & \\ & & & & \mathbf{c}_1 & \mathbf{c}_2 & & \\ & & & & & & \mathbf{c}_1 & \mathbf{c}_2 \end{pmatrix} \tag{2}$$

Then, the spreaded vectors of the pth sub-stream are given by:

$$\mathbf{D}_p \triangleq \left(\mathbf{d}_{p,1} \;\; \mathbf{d}_{p,2} \;\; \mathbf{d}_{p,3} \;\; \mathbf{d}_{p,4} \right) = \mathbf{C}\tilde{\mathbf{S}}_p \tag{3}$$

where

$$\mathbf{d}_{p,i} = \left(d_{p,i}^1 \;\; d_{p,i}^2 \;\; \cdots \;\; d_{p,i}^{4G} \right)^T, \quad i = 1,2,3,4 \tag{4}$$

denotes the sampled data flow with a period of $4T_S'$ belonging to the pth sub-stream assigned to the ith antenna. Note that the chip duration remains to be T_C, retaining the same bandwidth as that used in the full-rate STS based systems.

Using STS, each sub-stream is further split into N_T parallel flows assigned to N_T transmit antennas. At each antenna, a number of P flows perform frequency-domain interleaving with a depth of U, which duplicates each flow to U subcarriers with frequency space of $P \cdot \Delta$ to achieve the frequency-diversity, where Δ denotes the frequency separating interval between two adjacent subcarriers. Then, all $V = U \cdot P$ flows on each antenna modulate V different subcarriers by using the operation of V-point IFFT. The adjacent subcarrier frequency separating interval Δ is set to $1/T_C$, guaranteeing the orthogonal subcarrier condition. Then, after performing the Parallel-to-Serial (P/S) conversion, a cyclic prefix (CP) is added to eliminate the effect of inter-symbol interference (ISI). Finally, the signal is transmitted by the ith $(i = 1,2,...,N_T)$ antenna, see Fig. 1.

The transmitted signal $x_i(t)$ through the ith transmit antenna **Tx** i (see Fig. 1) within the block duration $4T_S'$ is determined by:

$$x_i(t) = \sqrt{\frac{P_T}{2N_T V}} \sum_{u=1}^{U} \sum_{p=1}^{P} \sum_{k=1}^{4G} d_{p,i}^k \, g\left(t - kT_C\right) \mathrm{e}^{j\frac{2\pi\left[(u-1)P+p\right](t-T_G)}{T_C}} \tag{5}$$

where $i = 1,2,...,N_T$; P_T denotes the total average transmission power; the coefficient $\sqrt{P_T/(2N_T V)}$ indicates that the system has the same total average power regardless of how many transmit antennas and subcarriers are used; the coefficient of 2 appearing in front of N_T in Eq. (5) is due to the fact that the half-rate STS scheme transmits each symbol twice at each antenna to satisfy the orthogonal design requirement; $d_{p,i}^k$ is given in Eq. (4); $g(t)$ is a normalized pulse shaping function which has the finite duration $[0, T_C)$ and T_G is the guard interval to generate cyclic prefix (CP).

Thus, the transmitted signals over all transmit antennas can be expressed in a vector form as follows:

$$\mathbf{x}(t) = \left(x_1(t) \;\; x_2(t) \;\; \ldots \;\; x_{N_T}(t) \right)^T . \tag{6}$$

B. Channel Model

The multipath Rayleigh channel impulse response $\tilde{h}_{i,j}(t,\tau)$ between the ith antenna at the transmitter and the jth antenna at the receiver can be characterized by

$$\tilde{h}_{i,j}(t,\tau) = \sum_{l=1}^{L_R} \alpha_{i,j}^l(t) \, \delta\left(\tau - \tau_{i,j}^l(t)\right) \tag{7}$$

where L_R denotes the number of resolvable paths; $\alpha_{i,j}^l(t)$ denotes the fading coefficient over the lth path, which is modeled as independent zero-mean complex-Gaussian process; and $\tau_{i,j}^l(t)$ denotes the delay of the lth path. We assume that the channel is frequency-selective, but the delay-spreads T_m of the channel satisfy $T_m \ll T_C$ such that each subchannel conforms to the flat fading. Thus, the vth subchannel frequency response $h_{i,j}^v(t)$ is determined by:

$$h_{i,j}^v(t) = \sum_{l=1}^{L_R} \alpha_{i,j}^l(t) \exp\left(-2\pi f_v \tau_{i,j}^l(t)\right) \tag{8}$$

where $v = 1,2,...,V$ and f_v denotes the center frequency of the vth subcarrier. Furthermore, the channel is assumed to be quasi-static, i.e., the fading coefficients are invariant over a block interval and vary from one block to another. Thus, during each block interval, the fading $h_{i,j}^v(t)$ can be denoted by $h_{i,j}^v[n]$, $n = 1,2,...$, where n is the discrete time index for the nth block interval. Since we focus on the discussion within a

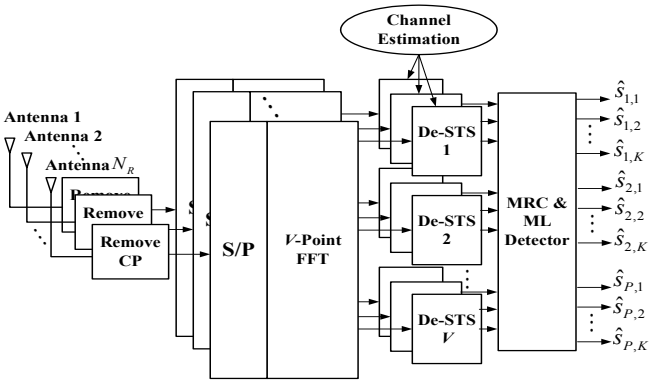

Fig. 2. Block diagram of the space-time spreading receiver.

block interval, we drop the time index n for simplicity in the rest of the paper.

As mentioned in Section II-A, the interleaving operation duplicates each input sub-stream to U subcarriers. We denote the U subchannel frequency responses corresponding to the pth input sub-stream, between the ith transmit antenna and the jth receive antenna, by $\left(h_{i,j}^{p,1} \quad h_{i,j}^{p,2} \quad ... \quad h_{i,j}^{p,U} \right)^T$. Under the condition where we appropriately select the system parameters, the subchannel responses $\left\{ h_{i,j}^{p,u} \,|u=1,2,...,U \right\}$ become independent. Specifically, $\left\{ h_{i,j}^{p,u} \,|u=1,2,...,U \right\}$ are independent if the frequency space $P \cdot \Delta$ between these interleaved subcarriers is larger than the coherent bandwidth of the channel, i.e. $P/T_C > 1/T_m$. Under such a condition, $\left\{ h_{i,j}^{p,u} \,|u=1,2,...,U \right\}$ can be modeled as i.i.d. complex-Gaussian variables with zero-mean and variance of $\Omega/2$ per dimension, i.e., $\Omega = E[\,|h_{i,j}^{v}|^2\,]$.

C. Receiver Model

The schematic of our proposed receiver is shown in Fig. 2. We assume that the channel information can be perfectly estimated by the receiver. First, we describe the decoding scheme for the case with $N_R = 1$ receive antenna. Then, we will generalize the scheme to the cases with more receive antennas.

The received signal $r(t)$ at the receive antenna can be expressed as follows:

$$r(t) = \sqrt{\frac{P_T}{2N_T V}} \sum_{i=1}^{N_T} \sum_{u=1}^{U} \sum_{p=1}^{P} h_i^{p,u} \sum_{k=1}^{4G} d_{p,i}^{k} g\left(t - kT_C\right) \times e^{j\frac{2\pi\left[(u-1)P+p\right](t-T_G)}{T_C}} + w(t) \tag{9}$$

where we drop the subscript j from the subchannel frequency response $h_{i,j}^{p,u}$ for simplicity (and similarly, we drop the other subscripts j from channel responses for the case of $N_R = 1$ receive antenna); and $w(t)$ is complex additive Gaussian white noise (AGWN) with variance equal to $N_0/2$ per dimension.

Performing the inverse operation of the transmitter, the receiver removes the cyclic prefix (CP), converts the serial data stream to V parallel flows (S/P), and conducts V-point FFT to obtain the frequency-domain signals. On the vth subcarrier, where $v = (u-1)P + p,\ \forall u = 1,2,...,U;\ \forall p = 1,2,...,P$, the sampled signal vector $\mathbf{r}_v$ at the receiver is determined by:

$$\mathbf{r}_v = \sqrt{\frac{P_T}{2N_T V}} \mathbf{D}_p \mathbf{h}_{p,u} + \mathbf{w}_v \tag{10}$$

where $\mathbf{D}_p$ is given in Eq. (3), $\mathbf{h}_{p,u} = \left(h_1^{p,u} \quad h_2^{p,u} \quad h_3^{p,u} \quad h_4^{p,u} \right)^T$, and $\mathbf{w}_v = \left(w_v^1 \quad w_v^2 \quad ... \quad w_v^{4G} \right)^T$ denotes frequency response of sampled $w(t)$ on the vth subcarrier. Then, the space-time de-spreading (De-STS) using the similar approach to [1] is applied at each subchannel. The decision variable $\mathbf{y}_v$ obtained from De-STS can be expressed as:

$$\mathbf{y}_v = \tilde{\mathbf{H}}_{p,u}^H \mathbf{C}^H \mathbf{r}_v \tag{11}$$

where

$$\tilde{\mathbf{H}}_{p,u} = \begin{pmatrix} \mathbf{H}_{p,u} \\ \mathbf{H}_{p,u}^* \end{pmatrix} \tag{12}$$

and

$$\mathbf{H}_{p,u} = \begin{pmatrix} h_1^{p,u} & h_2^{p,u} & h_3^{p,u} & h_4^{p,u} \\ h_2^{p,u} & -h_1^{p,u} & h_4^{p,u} & -h_3^{p,u} \\ h_3^{p,u} & -h_4^{p,u} & -h_1^{p,u} & h_2^{p,u} \\ h_4^{p,u} & h_3^{p,u} & -h_2^{p,u} & -h_1^{p,u} \end{pmatrix}. \tag{13}$$

Then, all U decision variables belonging to the pth input sub-stream are combined to achieve the frequency diversity, which is the procedure of maximal-ratio combining (MRC). The new decision variable $\mathbf{z}_p$ is specified by:

$$\mathbf{z}_p = \left(z_{p,1} \quad z_{p,2} \quad ... \quad z_{p,K} \right)^T = \sum_{u=1}^{U} \mathbf{y}_{(u-1)P+p}. \tag{14}$$

Substitute Eqs. (10)-(13) into Eq. (14) and apply the properties of the orthogonal design [1][6], we obtain $\mathbf{z}_p$'s expression as follows:

$$\mathbf{z}_p = \Theta_p \sqrt{\frac{2P_T}{N_T V}} \mathbf{I}_K \mathbf{s}_p + \mathbf{n}_p \tag{15}$$

where $\Theta_p = \sum_{u=1}^{U} \sum_{i=1}^{4} \left| h_i^{p,u} \right|^2$ is a random variable, $\mathbf{I}_K$ denotes the $K \times K$ identity matrix, and $\mathbf{n}_p$ is the noise vector with zero-mean and variance equal to $\Theta_p N_0$ per dimension. Thus, a diversity of $4U$ is achieved. In general, a diversity of $N_T U$ can be achieved by using N_T transmit antennas.

In case of more than one receive antennas, each receive block applies the same procedure and then sums up all the corresponding decision variables. Thus, random viable Θ_p in (15) becomes:

$$\Theta_p = \sum_{u=1}^{U} \sum_{i=1}^{N_T} \sum_{j=1}^{N_R} \left| h_{i,j}^{p,u} \right|^2 \tag{16}$$

through which a diversity of $UN_T N_R$ is achieved.

Finally, the maximum-likelihood (ML) detection to each symbol $\hat{s}_{p,k}$ is simplified as a linear processing, which is expressed by:

$$\hat{s}_{p,k} = \arg\min_{s \in S} \left\{ d^2\left(z_{p,k},\, s\right) \right\} \tag{17}$$

where S represents the entire symbol set, $d^2(a,b)$ denotes the square Euclidean distance between symbols a and b, and $z_{p,k}$ is the kth element of the vector $\mathbf{z}_p$.

III. Bit-Error Rate and Throughput Analysis

As mentioned in Section II-B, the subchannel fading factors $\left\{ h_{i,j}^{p,u} \,|u=1,2,...U \right\}$ are modeled as independent identical distributed (i.i.d.) complex-Gaussian variables with zero-mean and variance of $\Omega/2$ per dimension. Thus, the random variable

Θ (we drop the subscript p for simplicity) given in Eq. (16) follows χ^2 distribution with a degree of freedom $2UN_TN_R$. The probability density function $f(\theta)$ for Θ is given by:

$$f(\theta)=\begin{cases}\dfrac{\theta^{L-1}\mathrm{e}^{-\frac{\theta}{\Omega}}}{\Omega^L\Gamma(L)}, & \theta\geq 0\\ 0, & \theta<0\end{cases} \tag{18}$$

where $\Gamma(\bullet)$ denotes the gamma function and $L=UN_TN_R$.

In the following, we first derive the closed-form expressions of BER for a set of representative complex- and real-modulation based STS systems. Then, we derive the equation for the system throughput.

A. BER of M-ary PSK Modulation

From Eq. (15) and according to [5], the symbol error probability of M-ary PSK complex-modulation can be characterized by a random variable $\mathcal{P}_M$, which is specified by:

$$\mathcal{P}_M=2Q\left(\sqrt{\frac{2\Theta E_S}{N_0}}\sin\frac{\pi}{M}\right) \tag{19}$$

where $Q(\bullet)$ denotes the Q-function defined by:

$$Q(x)\triangleq\int_x^{+\infty}\frac{1}{\sqrt{2\pi}}e^{-\frac{t^2}{2}}dt \tag{20}$$

and E_S denotes the average transmission energy per symbol per subcarrier per antenna, namely:

$$E_S=\frac{P_T}{N_TV}(PT_S)=\frac{P_TT_S}{N_TU} \tag{21}$$

where PT_S denotes the symbol duration after S/P at the transmitter. When applying Gray-coding scheme [5], the bit-error probability can be well approximated by:

$$\mathcal{P}_b=\frac{1}{\log_2 M}\mathcal{P}_M \tag{22}$$

We calculate the BER as the expectation P_b of $\mathcal{P}_b$ with respect to the random variable Θ, which is determined by:

$$P_b=\frac{1}{\log_2 M}\int_0^{+\infty}2Q\left(\sqrt{\frac{2\theta E_S}{N_0}}\sin\frac{\pi}{M}\right)\frac{\theta^{L-1}\mathrm{e}^{-\frac{\theta}{\Omega}}}{\Omega^L\Gamma(L)}d\theta \tag{23}$$

Letting $\phi=\sqrt{2\theta/\Omega}$ and $\sigma=1\Big/\left(\sqrt{\bar{\gamma}_S}\sin\frac{\pi}{M}\right)$, where $\bar{\gamma}_S=E_S\Omega/N_0$, Eq. (23) can be rewritten as the following expression:

$$P_b=\frac{2^{2-L}}{\log_2 M\ \Gamma(L)}\int_0^{+\infty}\phi^{2L-1}\mathrm{e}^{-\frac{\phi^2}{2}}Q\left(\frac{\phi}{\sigma}\right)d\phi \tag{24}$$

Using the analytical property-35 of Q-function, see p.102 of [7], we can obtain the closed-form of the BER, i.e., P_b for M-ary PSK modulation, which is given by:

$$P_b=\frac{2}{\log_2 M}\left(\frac{1-\mu}{2}\right)^L\sum_{i=0}^{L-1}\binom{L+i-1}{i}\left(\frac{1+\mu}{2}\right)^i \tag{25}$$

where $\mu=\sqrt{\bar{\gamma}_S\sin^2\frac{\pi}{M}\Big/\left(1+\bar{\gamma}_S\sin^2\frac{\pi}{M}\right)}$.

B. BER of M-ary PAM Modulation

The symbol error probability expression of M-ary PAM is given by [5]:

$$\mathcal{P}_M=2\left(\frac{M-1}{M}\right)Q\left(\sqrt{\frac{6\Theta E_S}{\left(M^2-1\right)N_0}}\right) \tag{26}$$

Similarly, we need to calculate the expectation P_b of $\mathcal{P}_b$ with respect to the random variable Θ. We omit the derivations of P_b for lack of space. The BER P_b for M-ary PAM modulation is determined by:

$$P_b=\frac{2}{\log_2 M}\left(\frac{M-1}{M}\right)\left(\frac{1-\mu}{2}\right)^L\sum_{i=0}^{L-1}\binom{L+i-1}{i}\left(\frac{1+\mu}{2}\right)^i \tag{27}$$

where $\mu=\sqrt{3\bar{\gamma}_S\Big/\left(M^2-1+3\bar{\gamma}_S\right)}$ and $\bar{\gamma}_S=E_S\Omega/N_0$.

C. BER of M-ary QAM Modulation

The symbol error probability of M-ary QAM is determined by [5]:

$$\mathcal{P}_M=\left[1-\left(1-\mathcal{P}_{\sqrt{M}}\right)^2\right] \tag{28}$$

where $\mathcal{P}_{\sqrt{M}}$ represents the symbol error probability of $\sqrt{M}$-ary PAM. By employing the results of Eq. (27) obtained from Section III-B, we can derive the BER P_b for M-ary QAM modulation as follows:

$$P_b=\frac{1}{\log_2 M}\left[1-\left(1-P_{\sqrt{M}}\right)^2\right] \tag{29}$$

where

$$P_{\sqrt{M}}=2\left(\frac{\sqrt{M}-1}{\sqrt{M}}\right)\left(\frac{1-\mu}{2}\right)^L\sum_{i=0}^{L-1}\binom{L+i-1}{i}\left(\frac{1+\mu}{2}\right)^i \tag{30}$$

and $\mu=\sqrt{3\bar{\gamma}_S\Big/\left[2\left(M-1\right)+3\bar{\gamma}_S\right]}$ and $\bar{\gamma}_S=E_S\Omega/N_0$.

D. BER of BPSK Modulation

By applying the similar procedure used in the above, we can obtain the BER P_b for BPSK, which is given by:

$$P_b=\left(\frac{1-\mu}{2}\right)^L\sum_{i=0}^{L-1}\binom{L+i-1}{i}\left(\frac{1+\mu}{2}\right)^i \tag{31}$$

where $\mu=\sqrt{\bar{\gamma}_b/\left(1+\bar{\gamma}_b\right)}$ and $\bar{\gamma}_b=E_b\Omega/N_0$. Note that the similar expression of BER for BPSK modulation can also be found in [10], thus verifying the correctness of Eq. (31). However, the derivations of the BER for BPSK modulation in [10] differ from ours for Eq. (31).

E. System Throughputs

Applying the BER obtained above for different modulation schemes, we can derive the system throughput as follows. Let wireless data be transmitted in the unit of word, where each word consists of L_f bits. Then, the system throughput η can be characterized by the number of words which are correctly received per second. Under the assumption of independent losses/errors, the system throughput η can be expressed as follows:

$$\eta\triangleq R\left(1-P_b\right)^{L_f}=\frac{\log_2 M}{L_fT_S}\left(1-P_b\right)^{L_f} \tag{32}$$

where P_b is the BER determined by Eqs. (25), (27), (29), and (31), respectively, depending on which modulation scheme is used; and we define the system word-transmission rate R by:

$$R\triangleq\frac{\log_2 M}{L_fT_S} \tag{33}$$

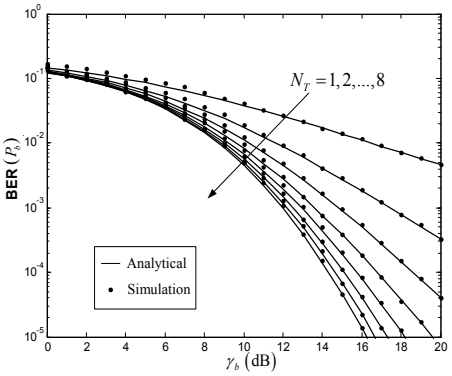

Fig. 3. BER of 16-QAM using different number of transmit antennas. The depth of interleaving $U = 1$; the number of receive antennas $N_R = 1$.

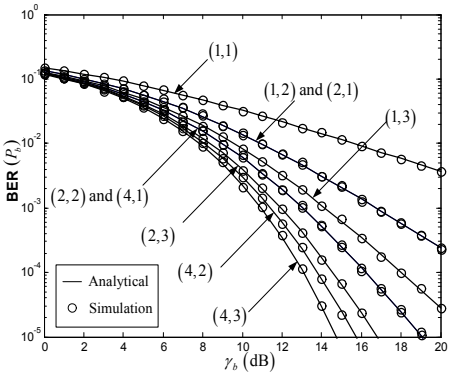

Fig. 4. The BER performance comparison between transmit diversity and frequency-interleaving with QPSK. The number of receive antenna $N_R = 1$.

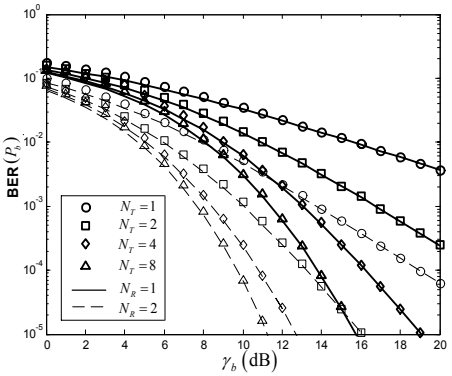

Fig. 5. The BER performance comparison between transmit diversity and receive diversity with 8-PSK modulation. The depth of interleaving $U = 1$.

where R varies as a function of M.

The variable $\overline{\gamma}_S$ used in Eqs.(25), (27), (29), and (31) for BER P_b, and indirectly used in Eq. (32) for throughput η, respectively, is the function of Signal-to-Noise-Ratio per bit γ_b, which is determined by:

$$\gamma_b = \frac{N_T U \overline{\gamma}_S}{\log_2 M} = \frac{N_T U \Omega E_S}{N_0 \log_2 M} \tag{34}$$

where $N_T U \Omega E_S / \log_2 M$ denotes the transmission energy per bit. Although this paper concentrates on half-rate STS based systems, the derivations described in this section can be applied to both full-rate and *any* non-full-rate STS based systems.

IV. Performance Evaluations and Comparisons

We use both analytical results derived in Section III and simulation experiments to evaluate the BER and throughput performance of our complex-modulation based STS MC-DS-CDMA systems. In all simulations, the spreading codes that we used are Walsh codes with spreading gain equal to $G = 32$. Also, we use Gray-coding for M-ary modulations. If the number of transmit antenna $N_T = 1$, then no STS scheme is applied; if the number of transmit antennas $N_T = 2$, then full-rate STS scheme is implemented. In all the figures, the symbols represent the results collected from simulation experiments and lines represent the numerical results obtained from analytical analyses.

Using Eq. (29), Fig. 3 plots the BER performance of 16-QAM versus SNR per bit γ_b with the number N_T of transmit antennas varying from 1 to 8 as indicated by the arrow. The number N_R of receive antenna and the depth U of interleaving are both set to 1. From Fig. 3, we observe that the BER performance is significantly improved by increasing N_T. For instance, about 5dB diversity gain can be achieved when N_T increases from 1 to 2 while setting BER equal to 10^{-2} and about 2.5dB diversity gain can be achieved when N_T increases from 2 to 3 with BER equal to 10^{-3}. However, when N_T becomes too large, the improvement rate starts dropping, which is because the system approaches to its maximum capacity. Thus, considering trade-off with the complexity of the system due to the increased N_T, Fig. 3 suggests that N_T not be larger than 8. Fig. 3 shows that the analytical results represented by lines agree well with the simulated results indicated by dot symbols, verifying the validities of our analytical results.

Employing Eq. (25), Fig. 4 compares the BER performance between transmit diversity and frequency-interleaving depth with QPSK modulation. The depth U of interleaving is set to 1, 2 and 3, and the number N_T of transmit antennas is set to 1, 2, and 4, respectively. In Fig. 4, we use digit pair (N_T, U) to denote that the specific line is drawn by using N_T transmit antennas and applying interleaving depth equal to U. Fig. 4, as well as the analytical analyses in Section III, shows that the diversity obtained from the increased numbers of transmit antennas and from frequency-interleaving has the same effect on BER performance. For example, the scheme with $N_T = 1$ and $U = 2$ denoted by (1,2) achieves the same BER as the scheme with $N_T = 2$ and $U = 1$ denoted by (2,1); also, $N_T = 4$ and $U = 1$ achieve the same BER as $N_T = 2$ and $U = 2$ when other conditions remain the same. One interesting question is: "can we just increase the depth of interleaving while keeping $N_T = 1$ unchanged since the two parameters have the same effect?" In fact, for a given symbol rate and system bandwidth, in order to guarantee the conditions of flat fading subchannels and independence of interleaved-repetitions described in Section II-B, the depth U is limited. Thus, we cannot merely increase the depth of interleaving to achieve the diversity without a limit. Again, the simulations confirm the analytical results, as shown by circle symbols being consistent with lines in Fig. 4.

Applying Eq. (25), Fig. 5 shows the BER performance comparison between transmit diversity and receive diversity with 8-PSK, where the solid and dotted lines represent analytical results for cases of $N_R = 1$ and $N_R = 2$, respectively, and the symbols with thicker and thinner drawings represent simulation results for cases of $N_R = 1$ and $N_R = 2$, respectively. The number N_T of transmit antennas is set to 1, 2, 4 and 8, and the number N_R of receive antennas is set to 1, 2, respectively. The depth of interleaving is set to $U = 1$. From Fig. 5, we observe that the scheme with $N_T = 1$ and $N_R = 2$ has 3 dB advantage in γ_b over the scheme with $N_T = 2$ and $N_R = 1$; the scheme with $N_T = 2$ and $N_R = 2$ has 3dB advantage in γ_b over the scheme with $N_T = 4$ and $N_R = 1$. These observations are consistent with the well known fact that the receive diversity has 3dB gain in γ_b over the transmit diversity [11], thus also verifying the correctness of our analyses derived in Section III. However, due to the complexity limitation of the mobile handset, the transmit diversity is practically more attractive. Fig. 5 also shows that the analytical results denoted by lines and simulation

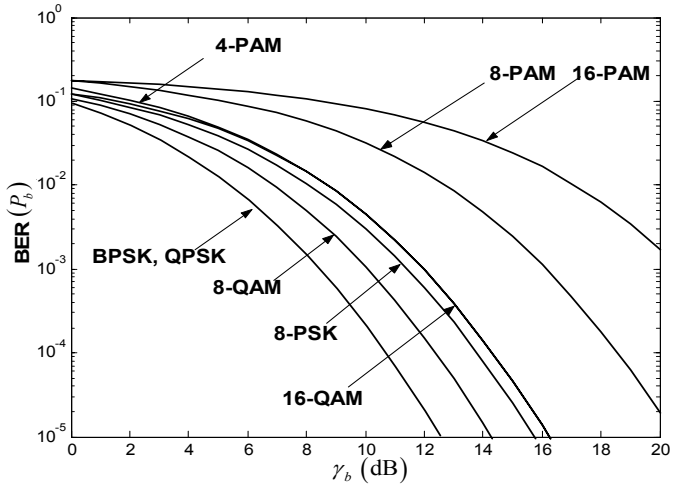

Fig. 6. The BER performance comparison of complex- and real-modulation based systems. The number of transmit antennas is $N_T = 4$ and the number of receive antenna is $N_R = 1$. The depth of interleaving $U = 2$.

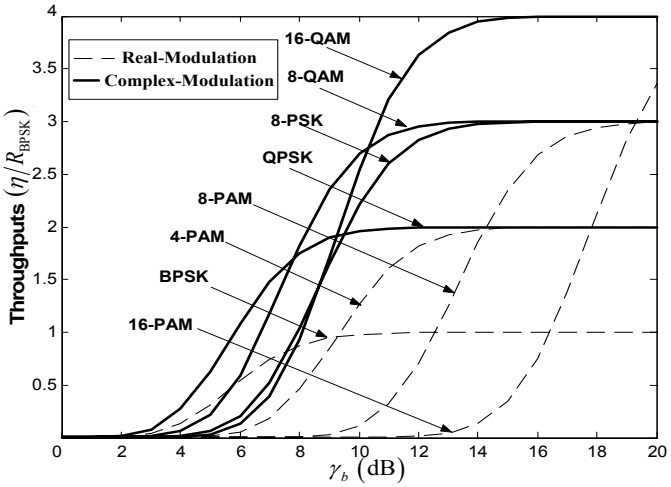

Fig. 7. Throughput performance comparison of complex- and real-modulation based systems. The number of transmit antennas is $N_T = 4$ and the number of receive antenna is $N_R = 1$. The depth of interleaving $U = 2$.

results denoted by various symbols agree well with each other, verifying the correctness of our analytical results.

Using BER equations derived in Section III, Fig. 6 presents the BER performance comparisons between complex- and real-modulation based STS schemes . The number of transmit antennas, the number of receive antennas, and the depth of interleaving are set to 4, 1, and 2, respectively. Since we have already verified in previous figures that the simulations and analytical results agree well, we only present numerical solution plots to evaluate the BER performance for simplifying presentation of Fig. 6 and Fig. 7. Using just one more spreading code than the real-modulation based STS, we can observe from Fig. 6 that the complex-modulation based STS schemes significantly outperform the real-modulation based schemes. For instance, about 6dB gain in γ_b can be achieved by employing 8-QAM instead of 8-PAM, and 9dB gain in γ_b can be achieved by using 16-QAM instead of 16-PAM given BER equal to 10^{-3} . On the other hand, if we need to maintain the same BER, the transmission rate of real-modulation based STS is lower than complex-modulation based STS. For example, BPSK and QPSK provide the exactly same BER performance but the bit rate of QPSK is 2 times higher than BPSK; 4-PAM and 16-QAM have very similar BER performance but the bit rate of 16-QAM is also 2 times higher than 4-PAM. Thus, our proposed system can provide higher transmission rate than the corresponding full-rate STS based systems given the same BER requirement.

Using Eqs. (32) and (33) and the same parameters as in Fig. 6, Fig. 7 plots the throughputs of different STS systems, where we set $L_f = 100$ bits. In Fig. 7, all throughputs (words/sec) are normalized by, i.e., divided by, BPSK's system word-transmission rate $R \triangleq R_{\text{BPSK}} = 1/(L_f T_S)$ (words/sec). We observe from Fig. 7 that all complex-modulation based STS schemes can achieve higher throughputs than the corresponding real-modulation based STS systems, given the same value γ_b of SNR per bit. In addition, as M increases, the improvement is more significant. For instance, to obtain the same system throughput, about 6dB gain in γ_b is achieved by using 8-QAM instead of 8-PAM, but about 9dB gain in γ_b is achieved by using 16-QAM rather than 16-PAM. When comparing the performance of different complex-modulation schemes, M-ary QAM generally outperforms M-ary PSK, e.g. 8-QAM has the better performance than 8-PSK, which can be observed from Fig. 6 as well.

V. Conclusion

We proposed a complex-modulation based space-time spreading scheme with more than two transmit antennas for MC-DS-CDMA systems, which significantly improve both spectrum efficiency and error performance. We also developed the performance analysis frameworks to evaluate the BER and throughput performance of our proposed scheme and the other existing schemes. Moreover, we conducted simulation experiments which verify the analytical results. Both analytical analyses and simulation experiments show that the proposed scheme can retain the same order of diversity as full-rate STS based systems. However, with just one extra spreading code, our proposed scheme can achieve much lower BER and much higher throughput as compared to its full-rate STS based counterparts, provided that the two systems have the same bandwidth capacity and the same transmission rate.

References

[1] B. Hochwald, T. Marzetta, and C. Papadias, "A Transmitter Diversity Scheme for Wideband CDMA Systems Based on Space-Time Spreading", *IEEE J. Select Areas Comm*., Vol. 19, Jan. 2001, pp. 48-60.

[2] J. Li, P. Fan, and Z. Cao, "Space-time Spreading in Forward Links of the Multicarrier DS CDMA System", *IEEE ICII*, Oct. 2001, pp. 285-290.

[3] C. Papadias, B. Hochwald, T. Marzetta, M. Buehrer and R. Soni, "Space-Time Spreading for CDMA Systems", 6th *Workshop on Smart Antennas in Wireless Mobile Communications*, Stanford, CA, Jul. 1999.

[4] R. Prasad and S. Hara, "Overview of multicarrier CDMA", *IEEE Commun. Mag*. pp. 126-133, Dec. 1997.

[5] J. Proakis, *Digital Communications*, 3rd Edition. New York: McGraw-Hill, 1995.

[6] V. Tarokh, H. Jafarkhani, and A. Calderbank, "Space-Time Block Codes from Orthogonal Designs", *IEEE Trans. Inform. Theory*, Vol. 45, No. 5, Jul. 1999, pp. 1456-1467.

[7] S. Verdu, *Multiuser Detection*, Cambridge University Press, 1998

[8] G. Wu, H. Wang, M. Chen, and S. Cheng, "Performance Comparison of Space-Time Spreading and Space-Time Transmit Diversity in CDMA2000", *IEEE* 54th *VTC*, Vol. 1, 2001, pp. 442-446.

[9] L-L Yang and L. Hanzo, "Space-Time Spreading Assisted Broadband MC-CDMA", *IEEE 55th VTC*, Vol. 4, 2002, pp. 1881-1885.

[10] ————, "Performance of Generalized Multicarrier DS-CDMA Over Nakagami-*m* Fading Channels", *IEEE Trans. Comm*., Vol. 50, No. 6, Jun. 2002, pp. 956-966.

[11] S. M. Alamouti, "A Simple Transmit Diversity Technique for Wireless Communications", *IEEE J. Select Areas Comm*., vol. 16, no. 8, Oct. 1998, pp. 1451-1458.